



Magnetically separable mesoporous silica-supported palladium nanoparticle-catalyzed selective hydrogenation of naphthalene to tetralin

Yonghui Yang^{1,2} | Bolian Xu^{1,3} | Jie He² | Jianjun Shi² | Lei Yu⁴ | Yining Fan^{1,3}

¹Key Laboratory of Mesoscopic Chemistry of Ministry of Education, School of Chemistry and Chemical Engineering, Nanjing University, Nanjing 210093, China

²School of Chemical Engineering, Anhui University of Science and Technology, Huainan 232001, China

³Nanjing University-Yangzhou Chemistry and Chemical Engineering Institute, Yangzhou 211400, China

⁴School of Chemistry and Chemical Engineering, Yangzhou University, Yangzhou 225002, China

Correspondence

Lei Yu, School of Chemistry and Chemical Engineering, Yangzhou University, Yangzhou 225002, China.
Email: yulei@yzu.edu.cn

Yining Fan, Key Laboratory of Mesoscopic Chemistry of Ministry of Education, School of Chemistry and Chemical Engineering, Nanjing University, Nanjing 210093, China.
Email: ynfan@nju.edu.cn

Funding information

National Natural Science Foundation of China, Grant/Award Number: 21773107; Priority Academic Program Development (PAPD) of Jiangsu Higher Education Institutions; Jiangsu Provincial Six Talent Peaks Project, Grant/Award Number: XCL-090; Natural Science Foundation of Jiangsu Province, Grant/Award Number: BK20181449; Natural Science Foundation of Yangzhou, Grant/Award Number: YZ2016137

A novel magnetically separable mesoporous silica-supported palladium catalyst was designed and prepared for the selective hydrogenation of naphthalene to tetralin, which is an important transformation from a practical viewpoint. In the catalyst, Pd nano grains were dispersed uniformly and protected within the mesoporous silica shells being coated on the Fe₃O₄ core, so that the durability of the catalyst could be significantly improved.

KEYWORDS

hydrogenation of naphthalene, magnetically separable catalyst, mesoporous silica, palladium, tetralin

1 | INTRODUCTION

Naphthalene is an ecotoxic molecule that abundantly exists in coal tar. Converting this chemical into useful products is meaningful from both environmental and

industrial viewpoints.^[1] In this regard, partial hydrogenation is a practical method to consume naphthalene because the product tetralin generated following this reaction is a useful industrial intermediate that is comprehensively used as a solvent in industrial production,

as an intermediate in agricultural chemical synthesis, and as a good hydrogen donor in fuel cells.^[2] In industrial catalysis, a variety of metal catalysts, such as Pd,^[3] Pt,^[4] Rh,^[5] Ru,^[6] Ir,^[7] and Ni,^[8] have been developed for the hydrogenation/dehydrogenation reactions, with alumina, zeolite, or activated carbon usually employed as the catalyst support.^[9] However, with the dwindling supplies of the metal resources in recent years, the cost of the catalyst is increasing. Therefore, developing easily recyclable and reusable catalyst for the transformation is crucial for industrial application purpose.

Nano catalysts have attracted much attention owing to their high efficiency as well as the green features of the reaction processes free of ligands or additives.^[10] In field applications, magnetic materials, such as Fe₃O₄, have been widely used as the support for catalytic metal nanoparticles (NPs) to achieve convenient magnetic separation as they enable more efficient catalyst recovery process, compared with the traditional homogeneous or heterogeneous catalysts.^[11] However, aggregation of active metal NPs may result in catalyst deactivation and is a major issue hindering their industrial application. To overcome this limitation, the use of magnetically separable mesoporous silica materials has been investigated,^[12] which afford additional opportunities to improve the related magnetic nano catalysts, in which the catalytic sites can be well protected within mesoporous silica shells to enhance the durability of the catalyst. However, there is no report on using a magnetic catalyst for naphthalene hydrogenation yet, let alone the application of magnetically separable mesoporous catalysts for the reaction. In most studies from our group, green reactions were utilized for synthesizing useful fine chemicals,^[13] and in this work, we chose to study the selective hydrogenation of naphthalene to tetralin due to its great significance in various industries. Recently, we developed a novel magnetically separable mesoporous silica-supported palladium nano catalyst (Fe₃O₄@SiO₂@mSiO₂-Pd) for the transformation.

2 | EXPERIMENTAL

2.1 | Materials

Iron (III) chloride hexahydrate, ethylene glycol, anhydrous sodium acetate, anhydrous ethanol, aqueous ammonia solution (28%), tetraethoxysilane (TEOS), cetyltrimethylammonium bromide (CTAB), acetone, hydrochloric acid, naphthalene, tridecane, and palladium chloride (PdCl₂) were purchased from Beijing Chemical Reagent Company (Beijing, China). All chemicals were of analytical grade and used directly without further purification. Deionized water was used in all experiments.

2.2 | Preparation of core-shell microspheres and catalyst

2.2.1 | Synthesis of Fe₃O₄ particles

About 2.7 g of FeCl₃·6H₂O and 7.2 g of anhydrous sodium acetate were added to 100 mL ethylene glycol to obtain a homogeneous yellow solution under magnetic stirring. The solution obtained was then placed in a Teflon-lined stainless-steel autoclave (200 mL) and sealed. After heating at 200 °C for 8 hr, the solution was cooled down to room temperature. The prepared Fe₃O₄ particles were magnetically separated, subsequently washed with water and ethanol, and dried in vacuum at 60 °C for 12 hr before use.

2.2.2 | Synthesis of Fe₃O₄@SiO₂@mSiO₂ core-shell microspheres

Fe₃O₄ particles weighing 0.10 g were immersed in 50 mL aqueous HCl (0.1 mol/L) for 10 min under ultrasonication conditions. The Fe₃O₄ particles were then washed with deionized water and dispersed in a mixture of ethanol (80 mL), deionized water (20 mL), and aqueous ammonia (1.0 mL; 28 wt%) under ultrasonication. Then, 0.03 g of TEOS was added to this mixture, which was subsequently stirred at room temperature for 6 hr. The microspheres thus obtained were separated and washed with ethanol and water, and re-dispersed in a mixed solution containing 0.30 g of CTAB, 80 mL of deionized water, 1.00 g of aqueous ammonia (28 wt%), and 60 mL of ethanol. The mixture was homogenized for 0.5 hr to obtain a uniform dispersion. TEOS (0.40 g) was then added dropwise into this dispersion with continuous stirring. After 6 hr, the product was magnetically separated and washed with ethanol and water to remove nonmagnetic by-products. Finally, CTAB templates in the materials were removed by extraction. During the process, the purified microspheres were re-dispersed in 60 mL of acetone and heated at a reflux temperature for 48 hr to remove the CTAB template. The aforementioned extraction process was repeated three times, and the microspheres obtained were washed with deionized water to produce the Fe₃O₄@SiO₂@mSiO₂ microspheres.

2.2.3 | Preparation of Fe₃O₄@SiO₂@mSiO₂-Pd

Fe₃O₄@SiO₂@mSiO₂ microspheres were immersed in an aqueous hydrochloric acid solution of PdCl₂ (PdCl₂ concentration was 5.6 × 10⁻³ mol/L and HCl concentration was 0.05 mol/L) at room temperature overnight. In this

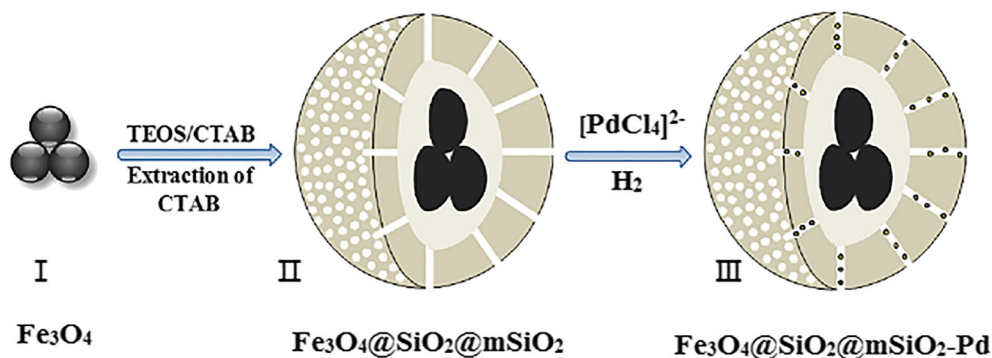


FIGURE 1 Diagram for the preparation of the core-shell-structured $\text{Fe}_3\text{O}_4@\text{SiO}_2@m\text{SiO}_2\text{-Pd}$ catalyst. CTAB, cetyltrimethylammonium bromide; TEOS, tetraethoxysilane

immersed into a palladium salt solution to load Pd^{2+} . Upon hydrogenation of the mixture, Pd^{2+} was reduced to Pd NPs, thus eventually generating the $\text{Fe}_3\text{O}_4@\text{SiO}_2@m\text{SiO}_2\text{-Pd}$ catalyst (**III**). The unique microstructure of the outer layer mesoporous channels in this material might facilitate adsorption and release of large-size guest objects during catalytic reactions.

3.2 | Characterization of catalyst

3.2.1 | X-ray diffraction analysis

XRD analysis was performed to characterize the as-prepared materials (Figure 2). In the wide-angle XRD pattern, signals of the high-crystalline cubic spinel structure of the as-prepared Fe_3O_4 agreed well with the standard Fe_3O_4 (cubic phase) XRD spectrum (Figure 2a, curve a, JCPDS 89-0688).^[14,15] The XRD pattern of $\text{Fe}_3\text{O}_4@\text{SiO}_2@m\text{SiO}_2$ microspheres prepared by the Stöber process is similar to that of Fe_3O_4 (Figure 2a, curve b vs. a), but an obvious diffraction peak at $2\theta = 15^\circ\text{--}25^\circ$, which was attributed to amorphous silica, was observed. In the XRD pattern of

$\text{Fe}_3\text{O}_4@\text{SiO}_2@m\text{SiO}_2\text{-Pd}$, both Fe_3O_4 and amorphous silica signals emerged (Figure 2a, curve c). Although inductively coupled plasma-mass spectrometry (ICP-MS) analysis indicated that the material contained about 1.96% of Pd, the characteristic peaks of Pd were not observed in its XRD pattern (Figure 2a, curve c), showing that the Pd NPs were well protected and dispersed uniformly inside the mesoporous silica shells. In the low-angle XRD patterns of the materials (Figure 2b, curves a-d), the (100) diffraction peaks at $2\theta = 2.4^\circ$ demonstrated that both $\text{Fe}_3\text{O}_4@\text{SiO}_2@m\text{SiO}_2$ and $\text{Fe}_3\text{O}_4@\text{SiO}_2@m\text{SiO}_2\text{-Pd}$ possessed mesoporous structures, which might be formed in the outer silica shell.^[14]

3.2.2 | N_2 adsorption-desorption experiments

N_2 adsorption-desorption experiments of the materials were performed and the isotherms are depicted in Figure 3. A linear increase was found in the amount of nitrogen adsorbed at a low relative pressure, which could be classified as a type of H2 hysteresis loop according to

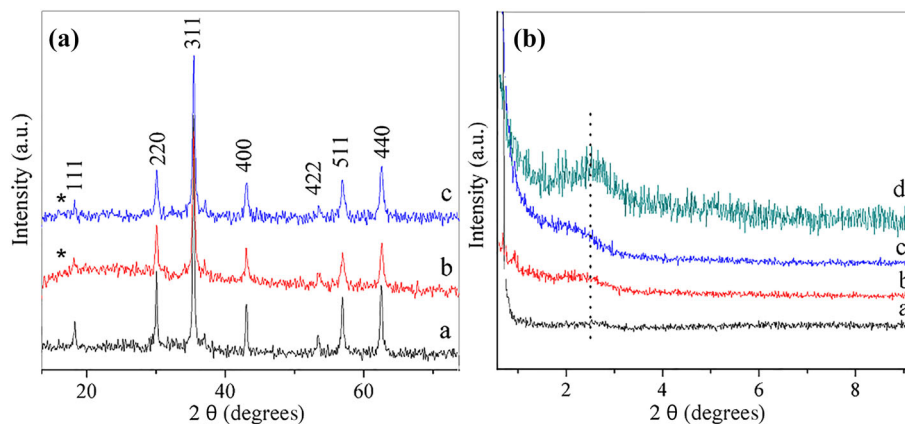


FIGURE 2 (a) Wide-angle X-ray diffraction (XRD) patterns and (b) low-angle XRD patterns of Fe_3O_4 particles (curve a), $\text{Fe}_3\text{O}_4@\text{SiO}_2@m\text{SiO}_2$ microspheres (curve b), $\text{Fe}_3\text{O}_4@\text{SiO}_2@m\text{SiO}_2\text{-Pd}$ catalyst (curve c), and pure mesoporous shell $m\text{SiO}_2$ (curve d)

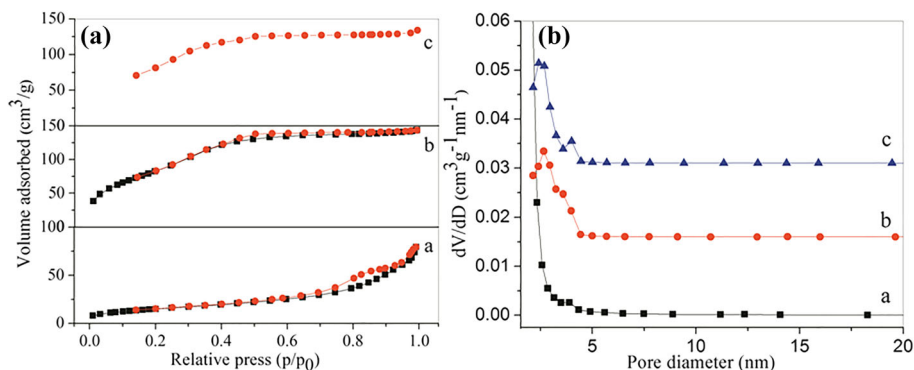


FIGURE 3 (a) N₂ adsorption–desorption isotherms and (b) pore-size distributions of Fe₃O₄ (curve a), Fe₃O₄@SiO₂@mSiO₂ (curve b), and Fe₃O₄@SiO₂@mSiO₂-Pd (curve c)

the IUPAC classification of physisorption isotherms and hysteresis loops.^[16] In the isotherms, both Fe₃O₄@SiO₂@mSiO₂ and Fe₃O₄@SiO₂@mSiO₂-Pd exhibited IV-type curves (Figure 3a, curves b and c). As calculated by the BJH method, the mesoporous size distribution of the materials exhibited sharp peaks centering on about 2.4–2.6 nm uniformly (Figure 3b, curves b and c). The specific surface areas of Fe₃O₄, Fe₃O₄@SiO₂@mSiO₂, and Fe₃O₄@SiO₂@mSiO₂-Pd were calculated to be 30, 313, and 302 m²/g, respectively, according to the BET method (see Table S1 in the supporting information). The related BJH desorption cumulative volumes of the aforementioned materials were 0.06, 0.26, and 0.24 cm³/g, respectively (see Table S1). The results showed that the silica coating dramatically enhanced both specific surface area (313 vs. 30 m²/g) and pore size (0.26 vs. 0.06 cm³/g) of the materials, whereas the loading of Pd NPs partially blocked the mesoporous channels and led to a slight decrease of the specific surface area (302 vs. 313 m²/g) and pore size (0.24 vs. 0.26 cm³/g) of the materials.

3.2.3 | Transmission electron microscopy analysis

The TEM images of Fe₃O₄, Fe₃O₄@SiO₂@mSiO₂, and Fe₃O₄@SiO₂@mSiO₂-Pd are presented in Figure 4. As

can be seen, the Fe₃O₄ particles were dispersed in a monolayer and had similar mean diameters (about 380 nm). They also had a spherical morphology and contained a cluster of magnetite NPs measuring about 20 nm, which are consistent with the result obtained using the Scherrer equation (Figure 4a). After treatment with the sol-gel approach based on the hydrolysis and condensation of TEOS, the mesoporous silica layer-covered core-shell-structured Fe₃O₄@SiO₂@mSiO₂ microspheres were obtained. The silica layer could be observed as the light borders around the Fe₃O₄ particles in the TEM image (Figure 4b). In Fe₃O₄@SiO₂@mSiO₂-Pd, the Pd NPs were embedded tightly within the silica layer on the surface of Fe₃O₄ core, and they were observed as small black dots in the light areas in the TEM image (Figure 4c).

3.2.4 | Magnetic features of the catalyst

The magnetic hysteresis loops indicated that the Fe₃O₄-cored materials possessed superparamagnetism (Figure 5 a). Both magnetization and demagnetization curves were consistent. No hysteresis phenomenon was observed, with the remnant magnetization and coercivity equaling zero. The maximum saturation magnetization of the as-prepared Fe₃O₄ was 82.2 emu/g (Figure 5a, curve a). The hysteresis loops of

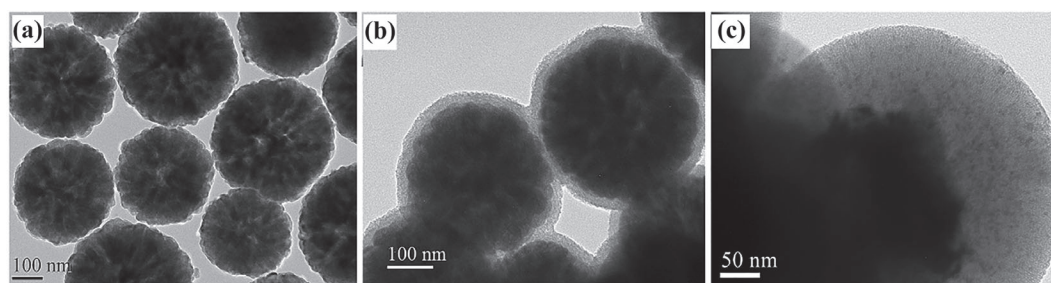


FIGURE 4 Transmission electron microscopy images: (a) Fe₃O₄, (b) Fe₃O₄@SiO₂@mSiO₂, and (c) Fe₃O₄@SiO₂@mSiO₂-Pd

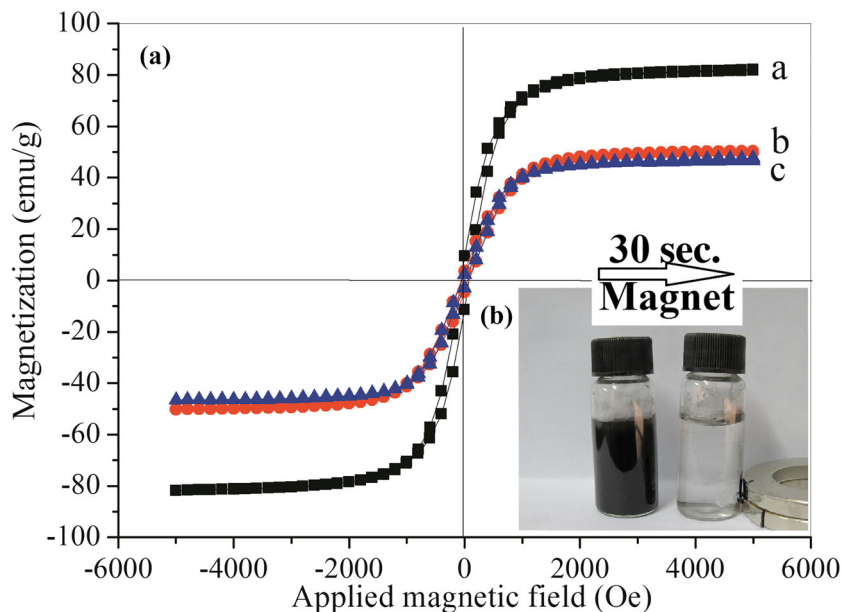


FIGURE 5 (a) Vibrating-sample magnetometer hysteresis loops: Fe_3O_4 (curve a), $\text{Fe}_3\text{O}_4@SiO_2@mSiO_2$ (curve b), and $\text{Fe}_3\text{O}_4@SiO_2@mSiO_2\text{-Pd}$ (curve c). (B) Photo of the separation process of the $\text{Fe}_3\text{O}_4@SiO_2@mSiO_2\text{-Pd}$ catalyst

$\text{Fe}_3\text{O}_4@SiO_2@mSiO_2$ and $\text{Fe}_3\text{O}_4@SiO_2@mSiO_2\text{-Pd}$ were substantially in accordance, showing that loading of Pd NPs did not affect the magnetic features of the material. Maximum saturation magnetizations of the mesoporous materials were 50.4 and 47.6 emu/g, respectively (Figure 5a, curves b and c). As shown in Figure 5b, the $\text{Fe}_3\text{O}_4@SiO_2@mSiO_2\text{-Pd}$ catalyst could be easily separated from the reaction liquid by a 30-sec external magnetic treatment.

3.3 | $\text{Fe}_3\text{O}_4@SiO_2@mSiO_2\text{-Pd}$ -catalyzed hydrogenation of naphthalene to tetralin

3.3.1 | Evaluation of catalyst performance

The hydrogenation reactions of naphthalene were performed over the $\text{Fe}_3\text{O}_4@SiO_2@mSiO_2\text{-Pd}$ material to evaluate its catalytic activity (Table 1). Upon heating 5 g of naphthalene with 0.1 g of catalyst in 120 mL of

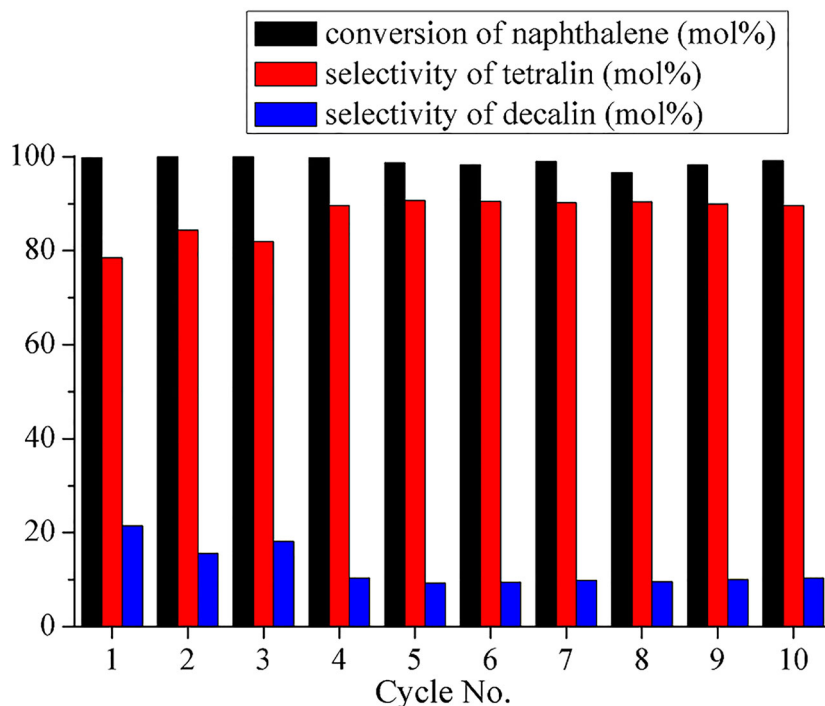


FIGURE 6 Recycling catalytic performance in hydrogenation of naphthalene over $\text{Fe}_3\text{O}_4@SiO_2@mSiO_2\text{-Pd}$ catalyst (reaction conditions: 120 mL of tridecane, 1 g of naphthalene, 0.3 g of the catalyst, $T = 240^\circ\text{C}$, $p = 6.5\text{ MPa}$)

tridecane solvent at 240 °C (pressure under 6.5 MPa H₂) for 3 hr, tetralin was obtained with 100% selectivity. About 19.1% of naphthalene was converted during the process (Table 1, entry 1). The reaction could be accelerated using higher volumes of the catalyst and extending the reaction time, which will increase the naphthalene conversion ratio (Table 1, entries 2 and 3). However, enhancing the initial concentration of naphthalene reduced its conversion ratio (Table 1, entry 4). By contrast, the conversion ratio of naphthalene was enhanced in reactions with reduced substrate concentration (Table 1, entries 5 and 6). The reaction with initial naphthalene concentration of 0.017 g/mL was found to be more preferable, yielding 96.9% tetralin; additionally, 3.1% of the over-reduction by-product decalin was produced (Table 1, entry 5).

3.3.2 | Catalyst recycle and reuse

As a magnetic catalyst, Fe₃O₄@SiO₂@mSiO₂-Pd could be easily separated following its use in the reaction and reused in subsequent reactions (Figure 5). The catalyst recycle and reuse experiments showed that the catalytic activity of this material could be well retained during the reaction processes (Figure 6). The hydrogenation reaction with the used catalyst could produce tetralin at yields of about 77%–90%, with the naphthalene substrate completely converted. Generation of the over-reduction by-product decalin was controlled to be within 20% yield. The catalyst was reused for at least 10 times without obvious deactivation and this should be attributed to the well-protected catalytic sites of Pd NPs by the outer layer mesoporous silica (Figure 6).

4 | CONCLUSION

In conclusion, we designed and prepared a magnetic mesoporous silica-supported palladium nano catalyst (Fe₃O₄@SiO₂@mSiO₂-Pd), in which double silica layers were coated over the magnetic Fe₃O₄ core. The active Pd NPs were dispersed uniformly and well protected within the outer layer mesoporous silica shells. The unique material structure facilitated the adsorption and mass transport of the molecules on its surface and enhanced the durability of the materials in catalysis circles. The as-prepared Fe₃O₄@SiO₂@mSiO₂-Pd was found to be an efficient and magnetically separable catalyst for selective hydrogenation of naphthalene to synthesize the useful product tetralin with excellent yield.

ACKNOWLEDGEMENTS

This work was supported by National Natural Science Foundation of China (21773107), Natural Science Foundation of Yangzhou (YZ2016137), Natural Science Foundation of Jiangsu Province (BK20181449), Jiangsu Provincial Six Talent Peaks Project (XCL-090), and Priority Academic Program Development (PAPD) of Jiangsu Higher Education Institutions.

ORCID

Lei Yu  <https://orcid.org/0000-0001-5659-7289>

References and Notes

- [1] a)H. Zhang, F. Zhu, X. Li, R. Xu, L. Li, J. Yan, X. Tu, *J. Hazard. Mater.* **2019**, *369*, 244. b)B. Large, N. Gigant, D. Joseph, G. Clavier, D. Prim, *Eur. J. Org. Chem.* **1835**, 2019. c)S. R. Barman, P. Banerjee, A. Mukhopadhyay, P. Das, *J. Environ. Chem. Eng.* **2017**, *5*, 4803. d)H. I. Abdel-Shafy, M. S. M. Mansour, *Egypt. J. Pet.* **2016**, *25*, 107. e)M. Usman, D. Li, R. Razzaq, M. Yaseen, C. Li, S. Zhang, *J. Ind. Eng. Chem.* **2015**, *23*, 21. f)K. Rao, R. G. Chaudhuri, S. Paria, *J. Environ. Chem. Eng.* **2014**, *2*, 826. g)C. Liang, A. Zhao, X. Zhang, Z. Ma, R. Prins, *Chem. Commun.* **2009**, *15*, 2047. h)S. R. Kirumakki, B. G. Shepizer, G. V. Sagar, K. V. R. Chary, A. Clearfield, *J. Catal.* **2006**, *242*, 319.
- [2] a)X. Chen, Y. Ma, L. Wang, Z. Yang, S. Jin, L. Zhang, C. Liang, *ChemCatChem* **2015**, *7*, 978. b)M. Pang, C. Liu, W. Xia, M. Muhler, C. Liang, *Green Chem.* **2012**, *14*, 1272. c)Y. Cheng, H. Fan, S. Wu, Q. Wang, G. Jin, L. Gao, B. Zong, B. Han, *Green Chem.* **2009**, *11*, 1061. d)Y. Wang, N. Shah, F. E. Huggins, G. P. Huffman, *Energy Fuels* **2006**, *20*, 2612.
- [3] Y.-F. Yang, M.-X. Li, H.-E. Cao, X. Zhang, L. Yu, *Mol. Catal.* **2019**, *474*, 110450.
- [4] a)F. Wang, L. Xu, C. Sun, L. Yu, Q. Xu, *Appl. Organomet. Chem.* **2018**, *32*, e4505. b)F. Wang, L. Xu, J.-J. Huang, S.-S. Wu, L. Yu, Q. Xu, Y.-N. Fan, *Mol. Catal.* **2017**, *432*, 99.
- [5] M. Siebels, C. Schlüsener, J. Thomas, Y.-X. Xiao, X.-Y. Yang, C. Janiak, *J. Mater. Chem. A* **2019**, *7*, 11934.
- [6] a)M. Jacquin, D. J. Jones, J. Rozière, S. Albertazzi, A. Vaccari, M. Lenarda, L. Storaro, R. Ganzerla, *Appl. Catal. A* **2003**, *251*, 131. b)A. C. Alves Monteiro-Gezork, R. Natividade, J. M. Winterbottom, *Catal. Today* **2008**, *130*, 471.
- [7] S. Albertazzi, R. Ganzerla, C. Gobbi, M. Lenarda, M. Mandreoli, E. Salatelli, P. Savini, L. Storaro, A. Vaccari, *J. Mol. Catal. A: Chem.* **2003**, *200*, 261.
- [8] X.-Y. Song, Q.-X. Guan, Y. Shu, X.-J. Zhang, W. Li, *ChemCatChem* **2019**, *11*, 1286.
- [9] a)M. Usman, L. Dan, R. Razzaq, U. Latif, O. Muraza, Z. H. Yamani, B. A. Al-Maythalony, C. Li, S. Zhang, *J. Environ. Chem. Eng.* **2018**, *6*, 4525. b)S.-Y. Zhao, B.-L. Xu, L. Yu, Y.-N. Fan, *Chin. Chem. Lett.* **2018**, *29*, 884. c)S.-Y. Zhao, B.-L. Xu, L. Yu, Y.-N. Fan, *Chin. Chem. Lett.* **2018**, *29*, 475. d)Y.-F. Yang, X. Fan, H.-E. Cao, S.-N. Chu, X. Zhang, Q. Xu, L. Yu, *Catal. Sci. Technol.* **2018**, *8*, 5017. e)K. Qian, A. Kumar, *Fuel* **2017**, *187*, 128. f)P. Gong, B. Li, X. Kong, J. Liu, S. Zuo, *Appl. Surf.*

- Sci.* **2017**, *423*, 433. g)H.-L. Zhou, J.-J. Gong, B.-L. Xu, S.-C. Deng, Y.-H. Ding, L. Yu, Y.-N. Fan, *Chin. J. Catal.* **2017**, *38*, 529. h)M. Pang, X. Chen, Q. Xu, C. Liang, *Appl. Catal. A* **2015**, *490*, 146.
- [10] a) M. Tinoco, S. Fernandez-Garcia, A. Villa, J. M. Gonzalez, G. Blanco, A. B. Hungria, L. Jiang, L. Prati, J. J. Calvino, X.-W. Chen, *Catal. Sci. Technol.* **2019**, *9*, 2328. b) C.-T. Qiu, Y.-S. Xu, X. Fan, D. Xu, T. Rika, X. Ling, Y.-N. Jiang, C.-B. Liu, L. Yu, W. Chen, C.-L. Su, *Adv. Sci.* **2019**, 201801403. c) H. Yan, C.-L. Su, J. He, W. Chen, *J. Mater. Chem. A* **2018**, *6*, 8793. d) Y.-J. Ai, Z.-N. Hu, Z.-X. Shao, L. Qi, L. Liu, J.-J. Zhou, H.-B. Sun, Q.-L. Liang, *Nano Res.* **2018**, *11*, 287. e) D.-L. Zhang, Z. Wei, L. Yu, *Sci. Bull.* **2017**, *62*, 1325. f) L. Yu, Z. Han, Y.-H. Ding, *Org. Process Res. Dev.* **2016**, *20*, 2124.
- [11] a)J.-C. Wang, R.-F. Nie, L. Xu, X.-L. Lyu, X.-Y. Lu, *Green Chem.* **2019**, *21*, 314. b)G. Pathak, K. Rajkumari, L. Rokhum, *Nanoscale Adv.* **2019**, *1*, 1013. c)A.-Q. Gao, H. Liu, L. Hu, H.-J. Zhang, A.-Q. Hou, K.-L. Xie, *Chin. Chem. Lett.* **2018**, *29*, 1301. d) M. N. Shaikh, M. A. Aziz, A. N. Kalanthoden, A. Helal, A. S. Hakeem, M. Bououdina, *Catal. Sci. Technol.* **2018**, *8*, 4709. e)Y.-M. Zhou, W.-T. Song, L.-J. Zhang, S.-Y. Tao, *J. Mater. Chem. A* **2018**, *6*, 12298. f)B.-L. Liu, H.-C. Zhang, Y. Ding, *Chin. Chem. Lett.* **2018**, *29*, 1725.
- [12] a)Z.-D. Wang, R.-Q. Wu, H.-M. Chen, N.-R. Sun, C.-H. Deng, *Nanoscale* **2018**, *10*, 5335. b)Q. Yue, J. Li, Y. Zhang, X. Cheng, X. Chen, P. Pan, J. Su, A. A. Elzatahry, A. Alghamdi, Y. Deng, D. Zhao, *J. Am. Chem. Soc.* **2017**, *139*, 15486. c)P. Cruz, Y. Perez, I. del Hierro, *Micropo. Mesopo. Mat.* **2017**, *240*, 227. d) L. Liu, Y.-J. Ai, D. Li, L. Qi, J.-J. Zhou, Z.-K. Tang, Z.-X. Shao, Q.-L. Liang, H.-B. Sun, *ChemCatChem* **2017**, *9*, 3131. e)J.-J. Zhou, Y.-N. Li, H.-B. Sun, Z.-K. Tang, L. Qi, L. Liu, Y.-J. Ai, S. Li, Z.-X. Shao, Q.-L. Liang, *Green Chem.* **2017**, *19*, 3400. f) X. Dong, X. Zhang, P. Wu, Y. Zhang, B. Liu, H. Hu, G. Xue, *ChemCatChem* **2016**, *8*, 3680. g)G. Cui, Z. Sun, H. Li, X. Liu, Y. Liu, Y. Tian, S. Yan, *J. Mater. Chem. A* **2016**, *4*, 1771. h)Q. Yue, Y. Zhang, C. Wang, X. Wang, Z. Sun, X. Hou, D. Zhao, Y. Deng, *J. Mater. Chem. A* **2015**, *3*, 4586.
- [13] a) X. Deng, H.-E. Cao, C. Chen, H.-W. Zhou, L. Yu, *Sci. Bull.* **2019**, *64*, 1280. <https://doi.org/10.1016/j.scib.2019.07.007> b)Y.-H. Zheng, A.-Q. Wu, Y.-Y. Ke, H.-E. Cao, L. Yu, *Chin. Chem. Lett.* **2019**, *30*, 937. c)S.-N. Chu, H.-E. Cao, T. Chen, Y.-C. Shi, L. Yu, *Catal. Commun.* **2019**, *129*, 105730. d)L. Yu, R.-R. Qian, X. Deng, F. Wang, Q. Xu, *Sci. Bull.* **2018**, *63*, 1010. e)H.-E. Cao, B.-R. Zhu, Y.-F. Yang, L. Xu, L. Yu, Q. Xu, *Chin. J. Catal.* **2018**, *39*, 899. f)L. Yu, Z. Han, *Mater. Lett.* **2016**, *184*, 312.
- [14] a)Y. Deng, Y. Cai, Z. Sun, J. Liu, C. Liu, J. Wei, W. Li, Y. Wang, D. Zhao, *J. Am. Chem. Soc.* **2010**, *132*, 8466. b)Y. Deng, D. Qi, C. Deng, X. Zhang, D. Zhao, *J. Am. Chem. Soc.* **2008**, *130*, 28.
- [15] C. Hui, C. Shen, J. Tian, L. Bao, H. Ding, C. Li, Y. Tian, X. Shi, H. Gao, *Nanoscale* **2011**, *3*, 701.
- [16] M. Thommes, K. Kaneko, A. V. Neimark, J. P. Olivier, F. Rodriguez-Reinoso, J. Rouquerol, K. S. W. Sing, *Pure Appl. Chem.* **2015**, *87*, 1051.

SUPPORTING INFORMATION

Additional supporting information may be found online in the Supporting Information section at the end of the article.

How to cite this article: Yang Y, Xu B, He J, Shi J, Yu L, Fan Y. Magnetically separable mesoporous silica-supported palladium nanoparticle-catalyzed selective hydrogenation of naphthalene to tetralin. *Appl Organometal Chem.* 2019;e5204. <https://doi.org/10.1002/aoc.5204>